

# A simple fully nonlinear Kirchhoff-Love shell finite element with thickness variation

Matheus L. Sanchez<sup>1</sup>, Catia C. Silva<sup>1</sup>, Paulo M. Pimenta<sup>1</sup>

<sup>1</sup> Polytechnic School at University of São Paulo

Av. Prof. Almeida Prado, trav.2 n°. 83 Edifício Paula Souza, 05424-970, São Paulo, Brazil

matheus.sanchez@usp.br, catia1@usp.br, ppimenta@usp.br

**Abstract.** The current paper develops a new multi parameter Kirchhoff-Love shell finite element with thickness variation able to reliably simulate thin nonlinear shell for static structural boundary value problems. The study is a continuation of previous elements developed in Sanchez et al [1] and Costa e Silva [2]. The element has 6 nodes and uses penalty (or optionally Lagrange method) to deal with the  $C_1$  continuity, which is a kinematical requirement of the Kirchhoff-Love shell model. It is also used a nonconform field of an incremental rotation variable  $\varphi_\Delta$  (this parameter is firstly introduced in Costa e Silva [2]) to assist with the  $C_1$  continuity on element edges. As a novelty in this study, the  $C_1$  continuity on the edges between elements is not further guaranteed by the maintenance of the kinking angle (as done in Viebahn et al [3]) or by the equivalence of  $\varphi_\Delta$  calculated through the displacements and the DoF shared by elements (as done in Sanchez et al [1] and Costa e Silva [2]). Now the  $C_1$  continuity is achieved by enforcing the transverse shear strain to zero. For the thickness variation, it is implemented a double linear non conform field similarly to Pimenta et al [4] to represent the quadratic displacement at transverse normal to midplane of the shell. The quadratic displacement field of the mid plane is represented as usual by the 6 parameters at the 6 nodes of the element.

**Keywords:** Finite element method, Kirchhoff-Love Shell, Thickness variation.

## 1 Introduction

Shell simulation in FEM is an important topic in research due to its application in structural engineering (slabs, domes, metal sheet, thin structures, for instance). When simulating very thin structures, one may face numerical difficulties with current finite element software. This problem is generally related to numerical unreal stiffness of the shell (or thin 3D domain) at finite element level, causing a phenomenon named “locking “. This is the main motivation of the development of the current model, and also the search for simplicity. This research is the continuation of previous work made by the group (see Sanchez et al [1], Costa e Silva [2], Viebahn et al [3], Pimenta et al [4], Campello et al [5] and Pimenta et al.[6]). In this paper, a new method for imposing  $C^1$  continuity is used based on the penalty (or Lagrange) of the shell shear strain.

## 2 Model Description

### 2.1 Shell Kinematics

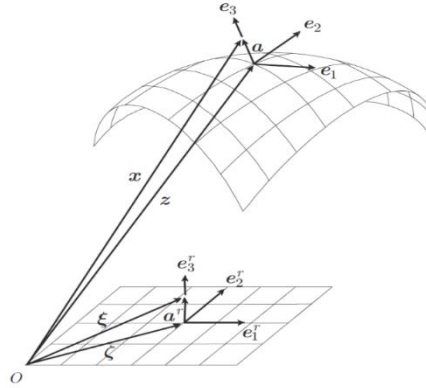


Figure 1 - Element Kinematic. Image Source Campello et al. [5]

The shell is based on Kirchhoff love model (Pimenta et al [6]), consequently some assumptions are made. Straight perpendicular lines to shell middle plane remain straight, do not change its length and are always perpendicular to the shell in any time (Reddy [7]).

The shell kinematics is defined by the following parametrization. Figure 1 may be of assistance. An arbitrary point in the shell at current time has its position defined by  $\mathbf{x} \in \mathbb{R}^3$  which may be decomposed in  $\mathbf{z} \in \Omega \subset \mathbb{R}^3$  (projection in shell middle surface) and  $\mathbf{a} \in \mathbb{R}^3$  (Perpendicular vector to middle surface). In the reference configuration, this same point position is represented by  $\xi \in \mathbb{R}^3$  which is also decomposed in  $\zeta \in \Omega^r \subset \mathbb{R}^3$  and  $\mathbf{a}^r \in \mathbb{R}^3$ . Here, it is assumed an initial plane reference configuration. According to Pimenta et al. [8], curved shells may be represented as an initial stress-free deformation. The following applies

$$\xi = \zeta + \mathbf{a}^r \quad , \quad \zeta = \xi_\alpha \mathbf{e}_\alpha^r, \quad \xi_\alpha \in \Omega^r \quad \text{and} \quad \mathbf{a}^r = \xi_3 \mathbf{e}_3^r, \quad \xi_3 \in H^r. \quad (1)$$

One may also define

$$\mathbf{x} = \mathbf{z} + \mathbf{a} \quad , \quad \mathbf{z} = \zeta + \mathbf{u} \quad , \quad \mathbf{a} = s \mathbf{e}_3 \quad , \quad \mathbf{e}_3 = \mathbf{Q} \mathbf{e}_3^r \quad \text{and} \quad \mathbf{Q} = \mathbf{e}_i \otimes \mathbf{e}_i^r. \quad (2)$$

A novelty in this research in comparison to previous work (Sanchez et al [1]) is the thickness variation of the shell. This is implemented using a new variable  $s$  which is used to define normal position  $\mathbf{a}$  of a point regarding middle plane. Then, one have

$$s = \hat{s}(\xi_3, p, q) = (1 + p)\xi_3 + \frac{1}{2}q\xi_3^2 \quad \text{and} \quad \begin{cases} p = \hat{p}(\xi_1, \xi_2) \\ q = \hat{q}(\xi_1, \xi_2) \end{cases}. \quad (3)$$

With previous definitions, it is possible to define the deformation gradient  $\mathbf{F}$  which is going to be used later to define deformation energy and the construct the Finite element. One has

$$\mathbf{F} = \partial \mathbf{x} / \partial \xi = \frac{\partial (\mathbf{z} + s \mathbf{Q} \mathbf{e}_3^r)}{\partial \xi_\alpha} \otimes \mathbf{e}_\alpha^r + \frac{\partial (\mathbf{z} + s \mathbf{Q} \mathbf{e}_3^r)}{\partial \xi_3} \otimes \mathbf{e}_3^r = \mathbf{f}_\alpha \otimes \mathbf{e}_\alpha^r + \mathbf{f}_3 \otimes \mathbf{e}_3^r. \quad (4)$$

One may yet define curvature vectors and tensor as

$$\begin{aligned} \mathbf{K}_\alpha &= \mathbf{Q}_{,\alpha} \mathbf{Q}^T & \boldsymbol{\kappa}_\alpha &= \boldsymbol{\Gamma}_\beta \mathbf{u}_{,\beta\alpha} \quad , \\ \boldsymbol{\kappa}_\alpha &= \text{axial}(\mathbf{K}_\alpha) \quad , & \text{and} \quad \boldsymbol{\Gamma}_1 &= (\mathbf{e}_1 \cdot \mathbf{z}_{,1})^{-1} [\text{Skew}(\mathbf{e}_1) - (\mathbf{e}_1 \cdot \mathbf{z}_{,2})(\mathbf{e}_2 \cdot \mathbf{z}_{,2})^{-1} (\mathbf{e}_1 \otimes \mathbf{e}_3)] \\ & & \boldsymbol{\Gamma}_2 &= (\mathbf{e}_2 \cdot \mathbf{z}_{,2})^{-1} (\mathbf{e}_1 \otimes \mathbf{e}_3) \quad . \end{aligned} \quad (5)$$

Previously, we have

$$\mathbf{f}_\alpha = \mathbf{z}_{,\alpha} + s_{,\alpha} \mathbf{Q} \mathbf{e}_3^r + s \mathbf{Q}_{,\alpha} \mathbf{e}_3^r = \mathbf{z}_{,\alpha} + s_{,\alpha} \mathbf{e}_3 + \boldsymbol{\kappa}_\alpha \times \mathbf{a} \quad \text{and} \quad \mathbf{f}_3 = s_{,3} \mathbf{Q} \mathbf{e}_3^r. \quad (6)$$

Defining the Back-rotated counterparts of  $\mathbf{F}$  and strains, we have

$$\mathbf{F}^r = \mathbf{Q}^T \mathbf{F} = \mathbf{I} + \boldsymbol{\gamma}_\alpha^r \otimes \mathbf{e}_\alpha^r + \boldsymbol{\gamma}_{33}^r \otimes \mathbf{e}_3^r \quad \text{and} \quad \begin{cases} \mathbf{e}_\alpha^r + \boldsymbol{\gamma}_\alpha^r = \mathbf{Q}^T (\mathbf{z}_{,\alpha} + s_{,\alpha} \mathbf{e}_3 + \boldsymbol{\kappa}_\alpha \times \mathbf{a}) \\ \mathbf{e}_3^r + \boldsymbol{\gamma}_{33}^r = \mathbf{Q}^T (s_{,3} \mathbf{e}_3) \end{cases}. \quad (7)$$

Then, consequently we have the strains at current and reference configurations defined by

$$\begin{cases} \boldsymbol{\gamma}_\alpha^r = \boldsymbol{\eta}_\alpha^r + \mathbf{k}_\alpha^r \times \mathbf{a}^r \\ \boldsymbol{\gamma}_{33}^r = (s_{,3} - 1) \mathbf{e}_3^r \end{cases} \quad \text{and} \quad \begin{cases} \boldsymbol{\eta}_\alpha^r = \mathbf{Q}^T \mathbf{z}_{,\alpha} + s_{,\alpha} \mathbf{e}_3^r - \mathbf{e}_\alpha^r \\ \mathbf{k}_\alpha^r = \text{axial}(\mathbf{Q}^T \mathbf{Q}_{,\alpha}) \end{cases} \quad (8)$$

$$\begin{cases} \boldsymbol{\gamma}_\alpha = \boldsymbol{\eta}_\alpha + \mathbf{k}_\alpha \times \mathbf{a} \\ \boldsymbol{\gamma}_{33} = (s_{,3} - 1) \mathbf{e}_3 \end{cases} \quad \text{and} \quad \begin{cases} \boldsymbol{\eta}_\alpha = \mathbf{z}_{,\alpha} + s_{,\alpha} \mathbf{e}_3 - \mathbf{e}_\alpha \\ \mathbf{k}_\alpha = \text{axial}(\mathbf{Q}_{,\alpha} \mathbf{Q}^T) \end{cases}.$$

## 2.2 Weak form of equilibrium and constitutive equations

The shell finite element model developed in this paper uses the virtual work theorem, then the following applies:

$$\delta W = \delta W_{int} - \delta W_{ext} = 0, \quad \forall \delta \mathbf{u} \quad \text{and} \quad \begin{cases} \delta W_{int} = \int_B \mathbf{P} : \delta \mathbf{F} dV = \int_{\Omega^r} (\boldsymbol{\sigma}_\alpha^r \cdot \delta \boldsymbol{\varepsilon}_\alpha^r) d\Omega^r \\ \delta W_{ext} = \int_{\partial B} \bar{\mathbf{t}} \cdot \delta \mathbf{x} dA + \int_B \bar{\mathbf{f}} \cdot \delta \mathbf{x} dV. \end{cases} \quad (9)$$

For convenience,  $\boldsymbol{\sigma}_\alpha^r$  and  $\boldsymbol{\varepsilon}_\alpha^r$  are defined by

$$\boldsymbol{\sigma}_\alpha^r = [\mathbf{n}_\alpha^r \quad \mathbf{m}_\alpha^r]^T \quad \text{and} \quad \boldsymbol{\varepsilon}_\alpha^r = [\boldsymbol{\eta}_\alpha^r \quad \mathbf{k}_\alpha^r]^T. \quad (10)$$

The equations above represent the balance of virtual work of external and internal forces ( $\delta w_{ext}$  and  $\delta w_{int}$ ), and  $\mathbf{k}_\alpha^r$  and  $\boldsymbol{\eta}_\alpha^r$  are Back-rotated curvature vector and membrane strains. Also,  $\bar{\mathbf{t}}$  and  $\bar{\mathbf{f}}$  are the boundary forces and  $\mathbf{n}_\alpha^r$  and  $\mathbf{m}_\alpha^r$  as Back-rotated Forces and moments per unit length.

The model is developed so far for an elastic material, which the following strain energy function applies

$$\psi = \frac{1}{2} \lambda \left( \frac{1}{2} (J^2 - 1) - \ln(J) \right) + \frac{1}{2} \mu (I_1 - 3 - 2 \ln(J)). \quad (11)$$

In the equation  $\psi(\mathbf{F})$  is Helmholtz free energy,  $\mathbf{C} = \mathbf{F}^T \mathbf{F}$  is deformation Cauchy-Green (right) tensor,  $\lambda$  and  $\mu$  are Lamé coefficients and  $I_i$  are the invariants of the Cauchy-Green tensor defined by

$$I_1 = \text{tr} \mathbf{C} = \mathbf{f}_i \cdot \mathbf{f}_i, \quad I_2 = \text{tr} [\text{Cof} \mathbf{C}] = \mathbf{g}_i \cdot \mathbf{g}_i, \quad I_3 = \det \mathbf{C} = J^2 = (\mathbf{f}_1 \cdot (\mathbf{f}_2 \times \mathbf{f}_3))^2. \quad (12)$$

## 2.3 Finite element definition

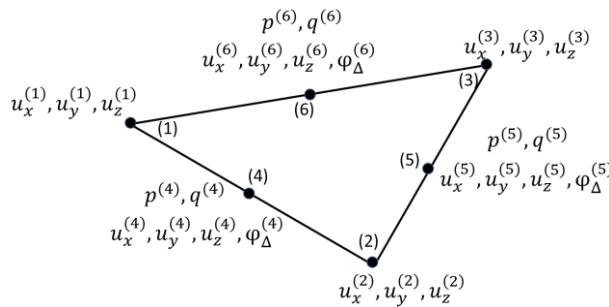


Figure 2 - Element field variables

Figure 2 represents the finite element and its field variables. It is a 6-node triangle with a standard quadratic displacement field. There are 3 scalar rotation parameters ( $\varphi_{\Delta}^{(4)}, \varphi_{\Delta}^{(5)}, \varphi_{\Delta}^{(6)}$ ) defined on the middle sides used for enforcing  $C^1$  continuity due to Kirchhoff-love hypothesis. Also, on the middle side nodes,  $p$  and  $q$  are defined to allow thickness variation of the shell similarly to Pimenta, P. M et al [4].

## 2.4 Enforcement of C1 Continuity

Due to Kirchhoff-love kinematical hypothesis, one may notice that the shear strain in any point on the middle plane of the shell is equal to zero. Inside the element it is guaranteed checking equation (8)

$$\boldsymbol{\eta}_{\alpha}^r \cdot \mathbf{e}_3^r = (\mathbf{Q}^T \mathbf{z}_{,\alpha} + s_{,\alpha} \mathbf{e}_3^r - \mathbf{e}_{\alpha}^r) \cdot \mathbf{e}_3^r = 0 \quad \text{and} \quad \boldsymbol{\eta}_{\alpha} \cdot \mathbf{e}_3 = (\mathbf{z}_{,\alpha} + s_{,\alpha} \mathbf{e}_3 - \mathbf{e}_{\alpha}) \cdot \mathbf{e}_3 = 0. \quad (13)$$

However, the continuity has been not guaranteed so far between adjacent elements. For this reason,  $\varphi_{\Delta}$  is implemented. One must make sure that both adjacent elements have compatible displacement fields in a way that the transverse shear strains remain equal to zero. This rotational-related variable will be used to build an unknown rotational tensor  $\mathbf{Q}_{\Delta}$  which is applied to an existing known rotational field  $\mathbf{Q}_i$  to create an end-of-step rotational tensor  $\mathbf{Q}_{i+1} = \mathbf{Q}_{\Delta} \mathbf{Q}_i$ . One can notice that so far there is no mechanism to enforce that  $\mathbf{Q}_{i+1}$  will make the end-of-step transversal strain  $\boldsymbol{\eta}_{\alpha} \cdot \mathbf{e}_3$  to be equal to zero. This may be understood because with the kinematical definitions of the shell model,  $\mathbf{Q}_{i+1}$  is no further defined as a function only of the displacements and enforced as perpendicular to the mid plane (as done in Matheus et al. [1]). Now,  $\mathbf{Q}_{i+1}$  is function of  $\varphi_{\Delta}$  and may create a state with transversal shear strain. Here the penalty method (or Lagrange multiplier) may be applied internally to the element to enforce the transversal shear strain to zero maintaining the Kirchhoff-love kinematical model. Using the new DOF, the system of both adjacent elements will be forced to use the same  $\varphi_{\Delta}$  variable and applying the penalty (or Lagrange), the system will be forced to adjust (numerically solving the system of equations) the unknown displacements to have the zero-transversal shear while keeping compatible rotational field.

Considering the share of  $\varphi_{\Delta}$  between adjacent elements, we have (as done in Costa e Silva [2])

$$\boldsymbol{\alpha}_{\Delta} = \|\mathbf{e}_3^m\|^{-2} (\mathbf{e}_3^i \times \mathbf{e}_3^{i+1}) + \varphi_{\Delta} \|\mathbf{e}_3^m\|^{-1} \mathbf{e}_3^m \quad \text{and} \quad \widehat{\mathbf{Q}}(\boldsymbol{\alpha}_{\Delta}) = \left( \mathbf{I} - \frac{1}{2} \mathbf{A}_{\Delta} \right)^{-1} \left( \mathbf{I} + \frac{1}{2} \mathbf{A}_{\Delta} \right) \quad (14)$$

with  $\mathbf{A}_{\Delta} = skew(\boldsymbol{\alpha}_{\Delta})$ .

Finally, it is used Penalty (or Lagrange multiplier) to enforce  $\boldsymbol{\eta}_{\alpha}^r \cdot \mathbf{e}_3^r = 0$  (or  $\boldsymbol{\eta}_{\alpha} \cdot \mathbf{e}_3 = 0$ ) at end of next iteration step. Consequently, we have to enforce

$$\mathbf{Q}_{\Delta} \mathbf{e}_3^i \cdot \mathbf{z}_{,\alpha}^{i+1} = 0 \quad \text{or} \quad \mathbf{Q}_{\Delta} \mathbf{e}_{\alpha}^i \cdot \mathbf{e}_3^{i+1} = 0 \quad (15)$$

to zero.

## 3 RESULTS

The finite element developed here has been implemented in AceGen / AceFEM platform (see Korelc and Wriggers [9]). It has been tested for some numerical examples to test it and to compare with other shell elements and commercial code (Autodesk Nastran CTRIA6 [10]). In this paper, it is presented the results for 3 numerical examples: Square simply supported Flat Plate subject to uniform load, Cantilever Beam and Cubic Stretching.

### 3.1 Square Flat Plate

In this example, the shell element has been tested to identify bending locking for a single linear step for different thickness. The square flat plate simple supported on 4 sides is defined with side  $L = 2m$ , Young modulus  $E = 10^6 \frac{kN}{m^2}$ , Poisson ratio  $\nu = 0,3$  and Center Down Pressure “ $q$ ” proportional to:  $q \approx h^3$ , and thickness  $h$ .

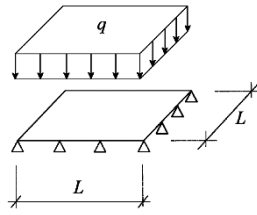


Figure 3 - Square Flat Plate. Source Campello et al [5]

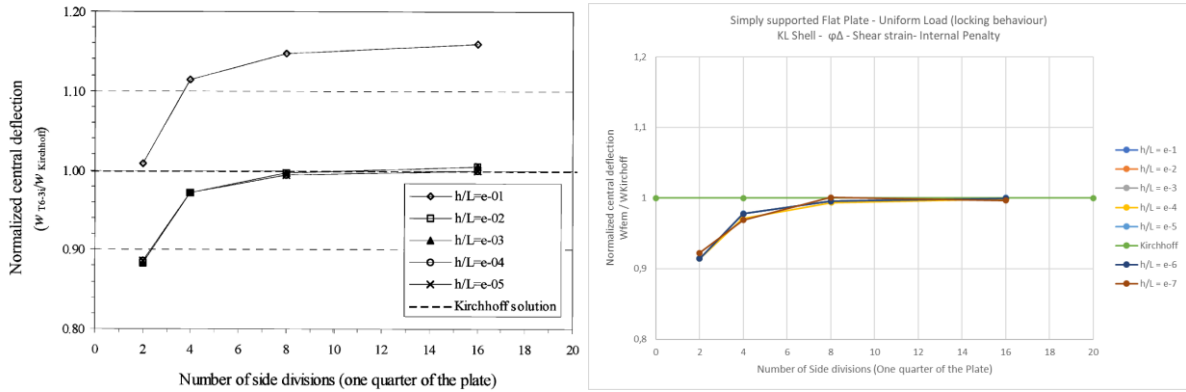


Figure 4 - Square Flat Plate results. (a) Campello et al. [5]; (b) current element.

The element was able to simulate for considerable thin shells with reliable results. Figure 4 shows the normalized results (numerical results divided by analytical Kirchhoff solution, see Young et al. [11]) for different meshes and thickness. It is important to mention that the element did not present locking behavior up to  $h/L = 10^{-7}$ . As a comparison, Campello et al. [5] had Non-locking behavior up to  $h/L = 10^{-5}$ .

### 3.2 Cantilever Beam

In this classical numerical example, a cantilever beam is subject to a bending force. See Figure 5. The beam has  $L$  (beam length) = 2400 mm,  $h$  (cross section height) = 100 mm,  $b$  (cross section width) = 11,64 mm,  $E$  (Elastic Modulus) =  $210 \cdot 10^9$  Pa,  $\nu$  (Poisson Ratio) = 0.3125. The Vertical applied force is  $F_y = 10000N$  and horizontal lateral force  $F_x = F_y \cdot 10^{-4}$ .

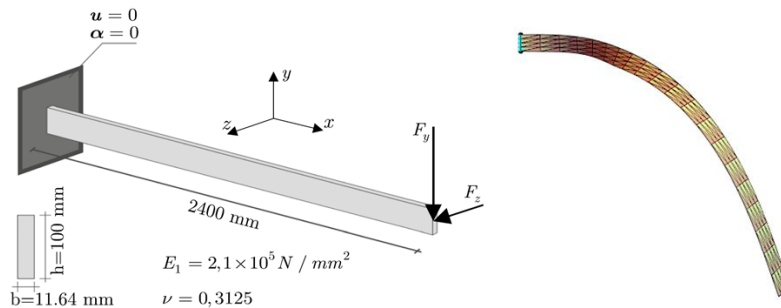


Figure 5 - Cantilever Beam

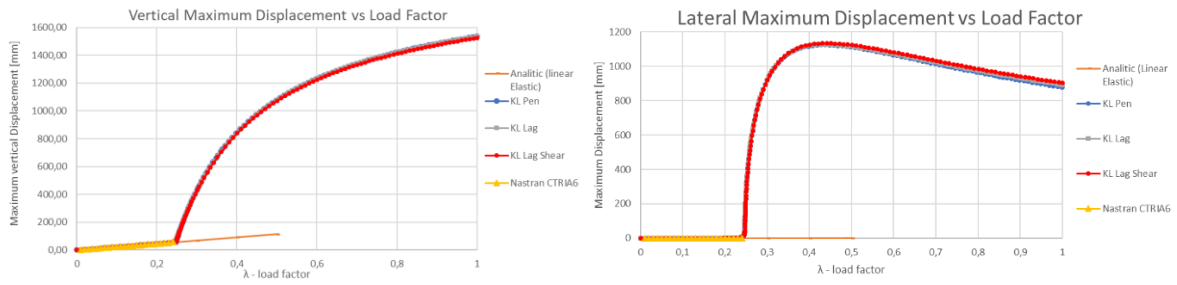


Figure 6 - Cantilever Beam (Non-Linear). Vertical and Horizontal displacement.

Figure 6 plots displacement of the free point of the cantilever beam. It can be observed that Nastran model could no converge for large loads (large displacements and rotations), and the results of the model in this article performance very similar to previous results (Sanchez et al [1]).

### 3.3 Cubic Stretching

This example is performance to study the capacity of the shell model to deal with stretching and consequently with thickness change. Here, a cube is approximated by the shell, considering side  $L = h = 1m$ , Elastic Modulus  $E = 10^5$ , Poisson Ratio  $\nu = 0.2, 0.4, 0.499$  and stretching force  $P = 0 \sim 200000N$ .

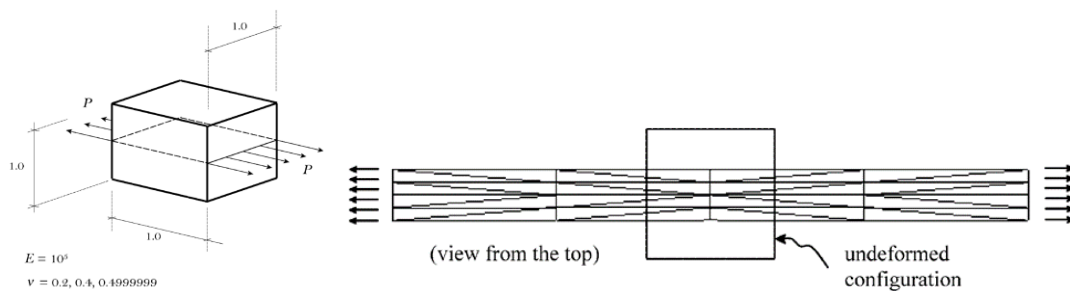


Figure 7 - Cubic Stretching. Image Source Pimenta et al.[4]

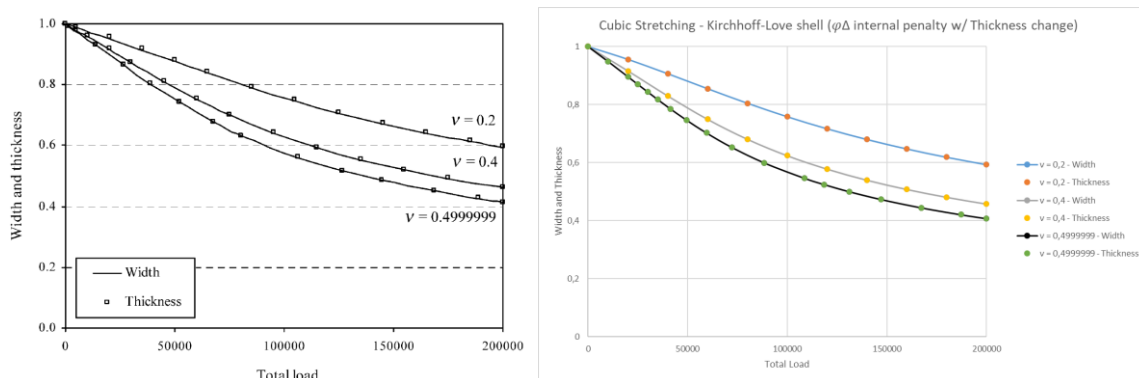


Figure 8 - Width and Thickness vs Poisson Ratios and loads. (a) Pimenta et al.[4] (b) Current shell model.

Figure 8 represents the stretching of the cube. Both width and thickness were evaluated as expected and similar to previous simulation (Pimenta et al.[4]).

## 4 Conclusions

The research results obtained so far demonstrates the reliability of the element developed. The authors believe that the simplicity of the kinematic in this geometrically exact nonlinear model, together with its capacity to simulate thin structures in large displacements, large rotations and for possibly different material models, makes this element appealing for further development. In further research yet to come, the authors are going to enhance the element for dynamic simulations and for non-isotropic materials (for example composites).

**Acknowledgements.** Matheus L. Sanchez thankfully acknowledges Clark Solutions, where he works as a project engineer providing financial support, knowledge, applicability and industrially experience. C. Costa e Silva gratefully acknowledges the Federal Institute of Science and Technology Education of São Paulo for financial support. P. M. Pimenta acknowledges the support by CNPq under the grant 308142/2018-7 and the Alexander von Humboldt Foundation for the Georg Forster Award that made possible his stays at the Universities of Duisburg-Essen and Hannover in Germany as well as the French and Brazilian Governments for the Chair CAPES-Sorbonne that made possible his stay at Sorbonne Universités on a leave from the University of São Paulo.

**Authorship statement.** The authors hereby confirm that they are the sole liable persons responsible for the authorship of this work, and that all material that has been herein included as part of the present paper is either the property (and authorship) of the authors or has the permission of the owners to be included here.

## References

- [1] Sanchez, M. L. et al., “A simple fully nonlinear Kirchhoff-Love shell finite element”. *Latin American Journal of Solids and Structures*, v.17, 2020.
- [2] Costa e Silva, C. “Geometrically exact shear-rigid shell and rod models”. Ph.D. Thesis, *Escola Politécnica da USP*, Brazil, 2020
- [3] Viebahn N. et al., “A simple triangular finite element for nonlinear thin shells: statics, dynamics and anisotropy”. *Computational Mechanics*, v. 59, n. 2, p. 281-297, 2017.
- [4] Pimenta, P. M et al., “A fully nonlinear multi-parameter shell model with thickness variation and a triangular shell finite element”. *Computational Mechanics*, v. 34, n. 3, p. 181-193, 2004.
- [5] Campello et al. “A triangular finite shell element based on a fully nonlinear shell formulation”. *Computational mechanics*, v. 31, n. 6, p. 505-518, 2003.
- [6] Pimenta, P.M., Neto, E.S.A, Campello E.M.B., “Fully Nonlinear Thin Shell Model of Kirchhoff-Love type”. *New trends in thin structures: formulation, optimization and coupled problems*. Springer, Vienna, p. 29-58, 2010.
- [7] Reddy, J. N., *Theory and analysis of elastic plates and shells*. CRC press, 2006.
- [8] Pimenta, P.M, Campello, E.M.B., “Shell curvatures as an initial deformation: a geometrically exact finite element approach”. *International journal for numerical methods in engineering*, v. 78, n. 9, p. 1094-1112, 2009.
- [9] Korelc, J.A., Wriggers, P. *Automation of Finite Element Methods. [S.l.]*. Springer, 2016.
- [10] Autodesk, Inc CTRIA6 Autodesk Nastran. “<https://knowledge.autodesk.com/support/nastran/learn-explore/caas/CloudHelp/cloudhelp/2020/ENU/NSTRN-Reference/files/GUID-956704D9-26C5-4FF8-85F2-955F383C5ECD-htm.html>”, 2019.
- [11] Young, W.C., Budynas, R.G., Sadegh, A.M., *Roark's formulas for stress and strain*. McGraw-Hill New York, 2002.